

STANDARD WATER PHANTOM BACKSCATTER FACTORS FOR MEDIUM ENERGY X-RAYS

M.A. HASSAN*, M.H. GABER**, E. ESMAT*, H.I. FARAG***, H.M. EISSA*

*National Institute for Standards (NIS), Giza, Egypt

**Biophysics Department, Faculty of Science, Cairo University, Egypt

***National Cancer Institute, Cairo, Egypt

Abstract. Experimentally determined values of X-ray backscatter factors were performed using NE 2571 cylindrical ionization chamber. Measurements were made for X-rays generated at voltages between 100 kV and 300 kV with different thickness and type of filters. To study the influence of the irradiation geometry on the backscatter factors, the measurements were performed for different photon beam field diameters at the phantom front face, at a fixed source-to-phantom distance of 1m. Measured results are analyzed and discussed in comparison with measured and calculated values given in the cited references.

Key Words: Backscatter factor, water phantom, X-ray, medium energy, beam quality index.

INTRODUCTION

After an initial decline in the use of the kilovolt (kV) X-ray units in radiotherapy departments, the use of these units has regained popularity during the last decade. This renewed interest in kV X-rays is clearly reflected in a number of recently issued kV X-ray dosimetry protocols [5, 6, 9, 11, 12]. All of these protocols use the Half Value Layer (HVL) as a sufficient beam quality index for medium energy X-ray. However, HVL does not uniquely define the quality of the beam as X-rays having a particular HVL may be produced either by light filtration of high-voltage radiation or by heavy filtration of low-voltage radiation. The aim of this work was to evaluate the HVL as adequate beam quality index for medium energy X-ray. Therefore, the experimental determination of the backscatter factor, as one of the important correction coefficients for the surface dose determination in medium energy X-ray, was performed from 100 to 300 kV for different the field diameters. Furthermore, studying the use of in-water dose ratio as an alternative beam quality index for medium energy X-ray [13] was performed in comparison with HVL.

Received February 2005,
in final form April 2005.

BACKGROUND

Experimental determination of the backscatter factor (*BSF*) based on an ionization technique requires a somewhat different approach although it is desirable to base the theoretical and experimental approaches on a similar formalism. Thus, the backscatter factor *BSF*, which defined as a water kerma ratio, can be written as

$$BSF = \frac{K_{air,s} [(\mu_{en} / \rho)_{w,air}]_s}{K_{air,f} [(\mu_{en} / \rho)_{w,air}]_f} \quad (1)$$

where $K_{air,s}$ is the air kerma that measured at the surface of the water phantom, $K_{air,f}$ is the air kerma at the same point in space in the absence of the phantom and $(\mu_{en} / \rho)_{w,air}$ is the ratio of the mass energy absorption coefficients for water and air in the presence of scattering medium and in free space.

In fact, the backscattering determined through the measurement of air kerma will have an uncertainty resulting from the unknown effect of the spectral distribution of the photon fluence, with and without the phantom, on the ratio of the mass energy absorption coefficients [8]. The magnitude of this uncertainty depends on how much the spectra differ. However, in 2002, Aoki and Koyama [1] have found the maximum difference between the backscatter factor defined as the ratio of air kerma and the backscatter factor defined as the ratio of water kerma to be 0.43%.

MATERIAL AND METHODS

The measurements of the *BSF* were performed in two steps. The first step was carried out for evaluating the effect of the Al filter thickness on *BSF*. While the second step was performed in order to compare between the effect of two different types of filters (Al and Cu) having the same thickness on the *BSF*. Table 1 represents the quality of the X-ray beam for performing the first step, whereas, the HVL was tabulated as a function of the applied kV for different thickness of additional Al filters. Table 2 demonstrates the beam quality parameters that used for the second step measurements. The first group was filtrated by Al filters, which was characterized as lower homogeneity coefficients – LHC (from 0.35 to 0.388), while the second group was filtrated by Cu filters, which was characterized by higher homogeneity coefficients – HHC (from 0.86 to 0.98).

Table 1

The HVL as a function of the applied kV for different additional Al filters at SSD 100 cm in air.

Generating potential in kV	HVL in mm Cu					
	Inherent filter	0.5 mm Al filter	1 mm Al filter	2 mm Al filter	4 mm Al filter	6 mm Al filter
100	0.00001	0.023	0.048	0.086	0.174	0.223
160	0.001	0.075	0.124	0.192	0.264	0.425
200	0.004	0.117	0.192	0.316	0.438	0.595
250	0.011	0.223	0.325	0.462	0.685	0.833
300	0.032	0.363	0.491	0.654	0.920	0.980

Table 2

Beam quality parameters determined at SSD 100 cm in air.

Beam energy in kV	Additional filter		HVL mm Cu		Homogeneity Coefficient (HC)	Beam quality group
	Al mm	Cu mm	I	II		
100	2		0.08	0.24	0.350	LHC
160	2		0.19	0.52	0.368	LHC
160	3		0.26	0.69	0.375	LHC
200	4		0.44	1.13	0.388	LHC
250	5		0.69	1.90	0.360	LHC
300	6		0.98	2.86	0.342	LHC
100		2	0.82	0.96	0.856	HHC
160		2	1.63	1.85	0.906	HHC
160		3	1.94	2.03	0.956	HHC
200		4	2.68	2.76	0.969	HHC
250		5	3.51	3.67	0.956	HHC
300		6	4.19	4.33	0.968	HHC

The IAEA water phantom (30×30×30 cm for horizontal beam) was used in this work as the scattering material [7]. The phantom was placed on the irradiation bench of the X-ray unit at a distance of 1 m from the beam focus. To mark the geometric center of the phantom and to measure the distance between the focus and the entrance phantom wall, a laser beam was used whose central axis coincided with that of the X-ray beam. The X-ray beam were collimated by a set of six collimating apertures, which were made of lead defined the opening angle of the beam. By using these collimating apertures circular fields were formed which had diameters of 5 cm, 7 cm, 10 cm, 15 cm, 20 cm and 50 cm at the surface of the phantom. The experimental arrangement was shown in Figure 1. The measurements of *BSF* were carried out using NE 2571 ionization chamber. Therefore, the inverse square correction for the air kerma between the chamber electrode and the surface

of the water phantom was performed. It was difficult in these measurements to estimate the scattering due to the chamber stem in case of the presence of the phantom and in free space for the used beam qualities. Although this effect was one of the sources of uncertainties in these measurements but it did not affect the aim of this work.

The uncertainty in the measurements was estimated to be $\pm 4.2\%$ at 95% confidence level, when the coverage factor equal 2.

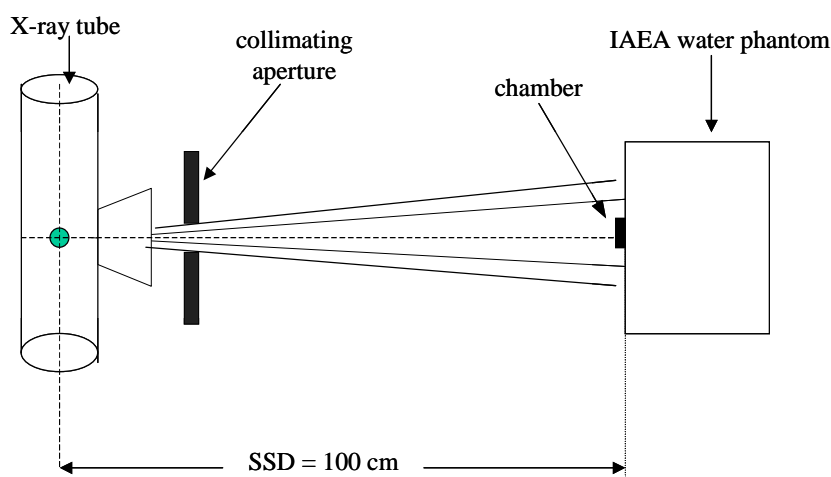


Fig. 1. Experimental arrangement for measuring backscatter factor.

RESULTS AND DISCUSSION

Figure 2 shows the relation between the field diameters and *BSF* for different X-ray beam energy at 100 cm source surface distance (SSD) for the inherent filtered beam. It was very clear the build up of the *BSF* with the field diameter. The Figure illustrates the effect of the field diameter on increasing *BSF* with different applied kV. It was also remarked that, when the field diameter was 5 cm, the difference between the *BSF* of the lower energy beam (100 kV) and higher (300 kV) was small, then it increased with the larger field diameters. This could be attributed to the increase in number of photons scattered back from the phantom as the field diameter increased [4].

Figure 3 shows the relation between the HVL and the *BSF* for 10 cm field diameter and 100 cm SSD. The values were obtained from the data that represented in Table 1. It was obvious that, *BSF* influenced by the thickness of the additional filters. Referring to the curve which represents the inherent filtrated beam in the

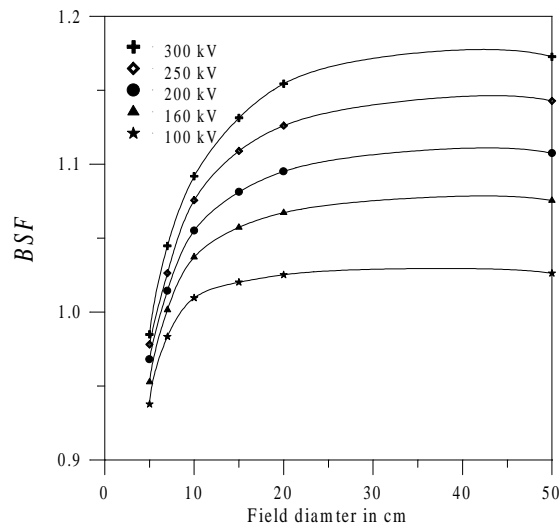


Fig. 2. The effect of field diameter on the backscatter factor from the water phantom for X-ray beam with inherent filter.

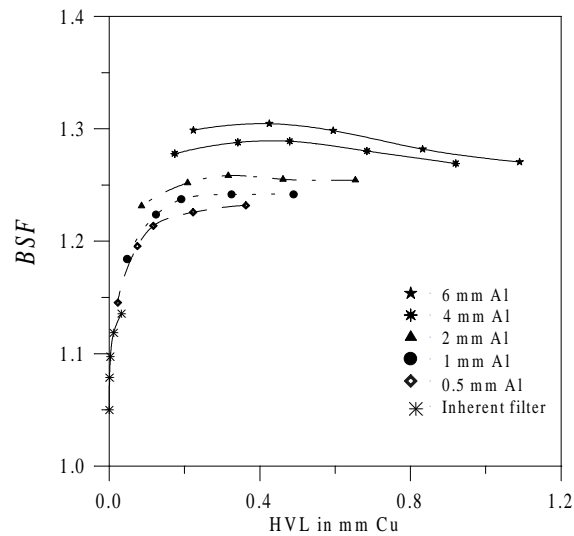


Fig. 3. The variation of the *BSF* with the filter thickness as a function of the HVL.

figure, the *BSF* increased with the HVL values which related to the applied kV values from 100 to 300 kV (as tabulated in Table 1). This could be attributed to the increase in the number of photons scattered back from the phantom as the increase in the X-ray spectrum energy. However, the obtained values of *BSF* were very small since, for the low HVL values the photoelectric absorption was the dominant interaction. By adding 0.5 mm Al filter, the *BSF* increased with HVL tending to be

constant at 0.2 mm Cu HVL. As a result of adding Al filter, the lower energy part of the X-ray beam spectrum was absorbed in the added filter. This reduced the probability of photoelectric absorption on surface of the phantom and increased probability of Compton scattering in comparing with the inherent filtrated beam. Furthermore, the *BSF* values increased with the addition of 1 mm Al filter.

Since the probability of absorbing the lower energy part of the X-ray spectrum increased by increasing the Al filter thickness. Therefore, *BSF* increased for the lower applied kV. Moreover, the softening of the beam occurred by increasing the applied kV (over 200 kV), which reduced the *BSF*.

Furthermore, the beam hardness was increased for the lower energy beam (less than 200 kV) by adding 2 mm Al filter as illustrated in Table1. Therefore the *BSF* values increased with the related HVL values in the Table. Whereas the Compton interaction at the surface of the phantom was the most probable for this lower energy beam and its probability could be equivalent to the higher energy beam softening (more than 200kV). This could explain the constancy in the obtained *BSF* values as a function of HVL in this curve. The addition of more Al filters (4mm and 6mm) increased the probability of Compton interaction for the lower energy and vice versa for the higher energy beam [14]. Therefore, in case of adding 4 and 6 mm Al filters, it was noted the decrease in the *BSF* with the HVL i.e. by increasing the applied kV for the same additional filters.

It was concluded that, different *BSF* values were obtained for a fixed HVL value. Thus, the HVL was not a good index for the obtained *BSF* values.

Figure 4 shows the experimental *BSF* from the water phantom as a function of the HVL at 10 cm field diameter and 100 cm SSD. There are two curves in the Figure; one illustrates the LHC group and the other HHC group. It was noted that, *BSF* went through a maximum at HVL between 0.5 and 5 mm Cu and went down rapidly at softer qualities i.e. low energies; this reflects the changeover from Compton scattering to photoelectric absorption as the dominant interaction mechanism when the energy falls [15]. In the LHC group the photoelectric interaction was the dominant, whereas this group was filtrated by the Al filters. Referring to Table 2, the HC of the LHC group increased till maximum values at 200 kV and 0.44mm HVL then it decreased once again for the next two beam qualities (250 kV & 0.69 mm HVL and 300 kV & 0.98 mm HVL). As a result of increasing in the Compton interaction, the *BSF* values increased till the maximum HC values in the LHC group. Then, *BSF* was decreased by decreasing the HC for the two next beam qualities which could be attributed to the softening of the higher energy X-ray spectrum (250 kV and 300 kV) as a result of penetration through 5mm and 6 mm Al filter respectively. On the other hand, the Compton interaction was the most important for the HHC beam quality group, which was filtrated by Cu filters. Whereas the maximum value of *BSF* was remarked at the beam quality 100 kV & 0.82 mm HVL then, *BSF* deceased as the HVL and HC increased. This was due to the increase in the beam hardness, which reduced the probability of scattered photon on the phantom surface.

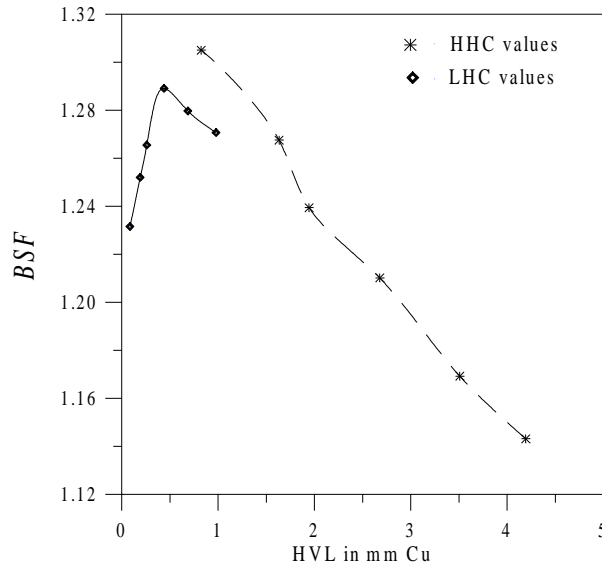


Fig. 4. The *BSF* as a function of the HVL for the beam quality groups (LHC and HHC) at 10 cm field diameter.

A comparison between the experimental *BSF* values and the *BSF* data given in the AAPM protocol [11] as a function of HVL was carried out. Figure 5 (a), (b), (c), and (d) represent the compared values for field diameters 20, 15, 10 and 5 cm respectively at 100 cm SSD. It was obvious that, the experimental values of LHC and HHC groups were always less than the AAPM values for the compared field diameters. In case of the LHC group, the maximum difference with the AAPM data was about 8.7% at 20 cm field diameter. However, the difference reduced as the field diameter decreased. Whereas, the minimum difference was about 2.5% at 5 cm field diameter. In case of the HHC group, the difference from the AAPM data was 4% at 20 cm field diameter and it was about 0.84% at 5 cm field diameter. It was also remarked that, the difference between the LHC group and the HHC group at 1 mm HVL reduced as the field diameter decreased. The maximum difference at 20 cm field diameter was about 5.3% while it decreased to 0.78% at 5 cm field diameter. By regarding the difference between the X-ray spectra between the compared values the differences are explainable [10].

In 1998, Rosser defined an alternative beam quality index that based on the in-water dose measurements. The index was defined as the ratio of dose at 2 and 5 cm depth in water. In the comment of the TRS-398 [6] about this topic, it stated that, the ratio of absorbed doses at 2 cm and 5cm depths in water is promising but needs further investigation. This ratio is likely to be related to the mean X-ray energy at the measurement depth in the phantom, which is potentially a better beam quality index than the HVL, measured in air.

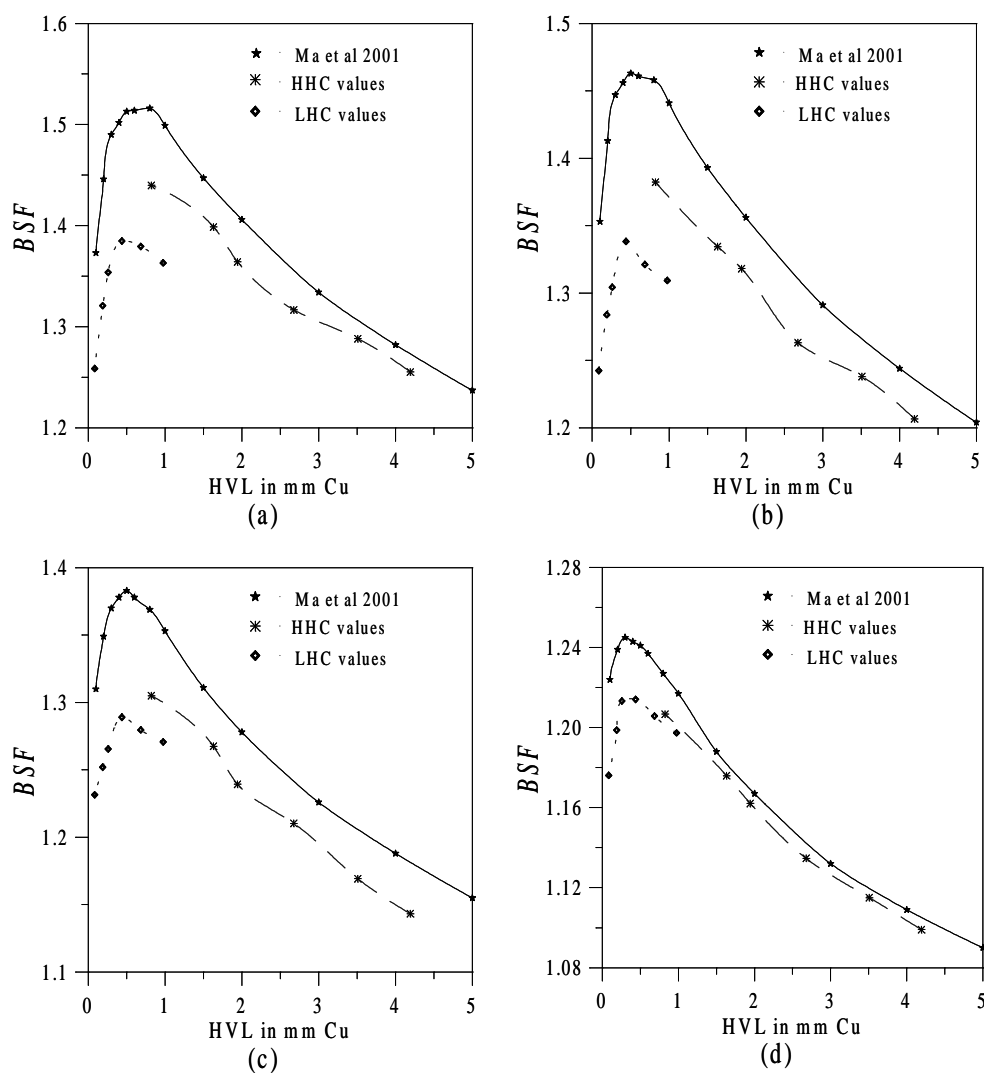


Fig. 5. A comparison between the *BSF* values for the beam quality groups (LHC and HHC) with the *BSF* data from the AAPM protocol [11] at 100 cm SSD and different field diameter: (a), (b), (c) and (d) represent the field diameter 20, 15, 10 and 5 cm, respectively.

Figure 6 shows the relation between the ratio of the dose at 2.5 cm to 5 cm ($D_{2.5}/D_5$) (whereas, the measuring depth in the IAEA water phantom start from 2.5 cm) and the *BSF* for different applied kV at 10 cm field diameter. It was remarked that, there was a unique *BSF* value for each value of the ratio $D_{2.5}/D_5$. Comparing with the Figure 3., the ratio $D_{2.5}/D_5$ is more convenient for the user for best definition of the medium energy X-ray beam qualities rather than the HVL.

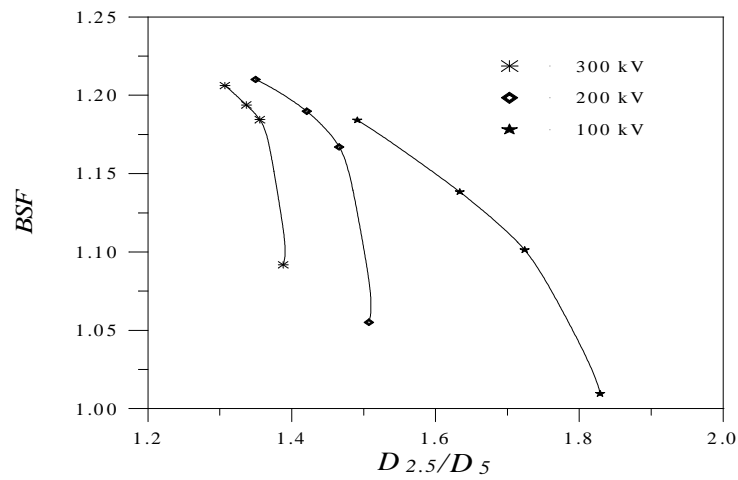


Fig. 6. The backscatter factor BSF as a function of the in-water dose ratio $D_{2.5}/D_5$.

Figure 7 shows the expansion of the in-water dose ratio interval against the BSF when using the ratio at 5 cm to 10 cm (D_5/D_{10}). This increase in the in-water dose ratio obtained a wide range to use the ratio as a beam quality index for medium energy X-ray.

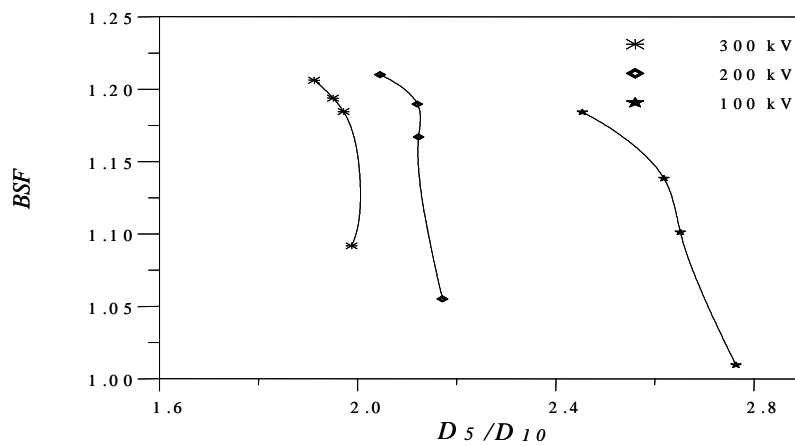


Fig. 7. The BSF as a function of the in-water dose ratio D_5/D_{10} .

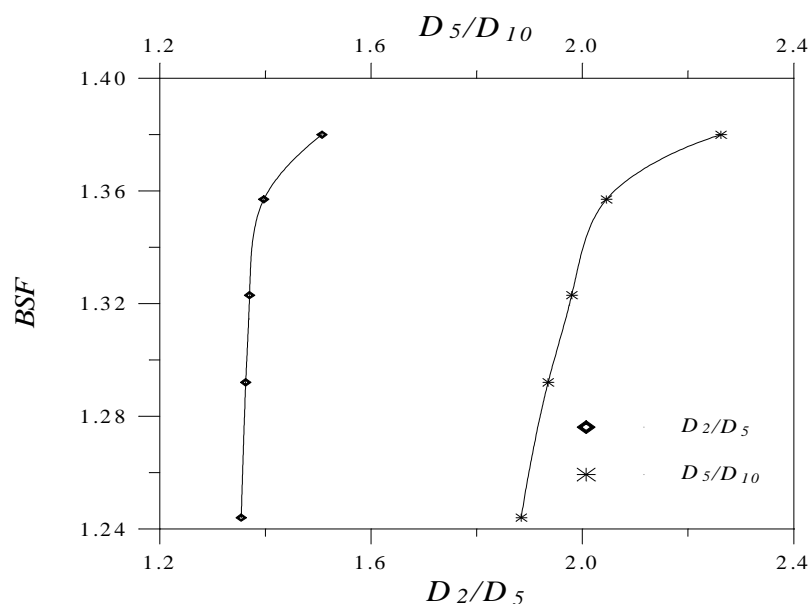


Fig. 8. The difference between the intervals of D_2/D_5 ratio and D_5/D_{10} ratio against the BSF .

For further investigation, Figure 8 shows the difference between interval of the D_2/D_5 and D_5/D_{10} against the BSF for supplement 25 [3] data (from 0.5 to 3 mm Cu HVL at 10x10 cm field size). It was obvious that, the wider range was obtained for the ratio D_5/D_{10} than the ratio D_2/D_5 and it was more convenient to obtain a definite value for the BSF when using D_5/D_{10} ratio.

CONCLUSION

There are different BSF values for the same HVL, as a result of using different applied kV and beam filtration. However, the use of a small field diameter reduces the variation in BSF due to the difference in the quality of the beam for the same HVL. The results demonstrate the difficulty in obtaining a constant value for the BSF based on the HVL as the beam quality index and neglecting the applied kV. The use of in-water dose ratio as an alternative beam quality index for medium energy X-ray gives better definition about the beam quality in water. The dose ratio at 5 cm to 10 cm in water has the wider range values than the ratio 2 cm to 5 cm for defining the BSF . Furthermore, the in-water dose ratio is likely to be related to the mean X-ray energy at the measurement depth in water, which is potentially a better beam quality index than the HVL, measured in air.

REFERENCE

1. AOKI, K., M. KOYAMA, Measurement of backscattered X-ray spectra at water surface in the energy range 60 kV to 120 kV, *Phys. Med. Biol.*, 2002, **47**, 1205–1217.
2. BJR, Central axis depth dose data for use in Radiotherapy, *Br. J. Radiol.*, Supplement, **25**, The British Institute of Radiology, London, 1996.
3. CARLSSON, C.A., Differences in reported backscatter factors for low-energy X-ray: a literature study, *Phys. Med. Biol.*, 1993, **38**, 521–531.
4. GROSSWENDT, B., Dependence of the photon backscatter factor for water on source-to-phantom distance and irradiation field size, *Phys. Med. Biol.*, 1990, **35**, 1233–1245.
5. *International Atomic Energy Agency (IAEA)*, Absorbed dose determination in photon and electron beams: an international code of practice, *IAEA Technical Reports Series no. 277*, 2nd ed., Vienna: IAEA, 1997.
6. *International Atomic Energy Agency (IAEA)*, Absorbed dose determination in external beam radiotherapy: An international code of practice for dosimetry based on standards of absorbed dose to water, *IAEA Technical Reports Series no. 398*, Vienna: IAEA, 2000.
7. *International Commission on Radiation Units and Measurements (ICRU)*, Phantom and computational models in therapy, diagnosis and protection, *ICRU Report No. 48*, ICRU, Washington D.C., 1992.
8. KLEVENHAGEN, S.C., Experimentally determined backscatter factors for X-rays generated at voltages between 16 and 140 kV, *Phys. Med. Biol.*, 1989, **34**, 1871–1882.
9. KLEVENHAGEN, S.C., R.J. AUKETT, R.M. HARRISON, C. MORETTI, A.E. NAHUM, K.E. ROSSER, The IPEMB code of practice for the determination of absorbed dose for X-rays below 300 kV generating potential (0.035 mm Al – 4 mm Cu HVL; 10–300 kV generating potential), *Phys. Med. Biol.*, 1996, **41**, 2605–2625.
10. KNIGHT, R.T., Backscatter factors for low- and medium-energy X-rays calculated by Monte Carlo method, *Royal Marsden NHS Trust Internal Report ICR-Phys-1*, **93**, 1993.
11. MA, C.M., C.W. COFFEY, L.A. DEWERD, C. LIU, R. NATH, S.M. SELTZER, J.P. SEUNTJENS, *AAPM TG61* AAPM protocol for 40–300 kV X-ray beam dosimetry in radiotherapy and radiobiology, *Med. Phys.*, 2001, **28**, 868–894.
12. NCS, Dosimetry for low and medium energy X-rays: a code of practice in radiotherapy and radiobiology” *NCS Report 10*, Delft: Netherlands Commission on Radiation Dosimetry, 1997.
13. ROSSER, K. E., An alternative beam quality index for medium energy X-ray dosimetry, *Phys. Med. Biol.*, 1998, **43** 587–598.
14. VERHAEGEN, F., A.E., NAHUM, S. VAN DE PUTTE, Y., NAMITO, Monte Carlo modelling of radiotherapy kV X-ray units, *Phys. Med. Biol.*, 1999, **44**, 1767–1789.
15. ZAIDI, H., G. SGOUROS (Eds), *Therapeutic Applications of Monte Carlo Calculations in Nuclear Medicine*, Institute of Physics Publishing, Bristol and Philadelphia, 2003.